THESIS FOR THE DEGREE OF LICENTIATE OF ENGINEERING

On motion resistance estimation and modeling for heterogeneous road vehicles

Mikael Askerdal

CHALMERS
UNIVERSITY OF TECHNOLOGY

Department of Electrical Engineering
Chalmers University of Technology
Gothenburg, Sweden, 2023

On motion resistance estimation and modeling for heterogeneous road vehicles

Mikael Askerdal

This thesis has been prepared using LaTeX.

Department of Electrical Engineering
Chalmers University of Technology
SE-412 96 Gothenburg, Sweden
Phone: +46 (0)31 772 1000
www.chalmers.se

Printed by Chalmers Reproservice
Gothenburg, Sweden, January 2023

To my beloved children Hugo and Lova.

Abstract

Climate change is driving the development of CO_2 reducing technologies within the transportation industry. One of the most promising technologies is battery electric vehicles. However, the combination of limited battery capacity, relatively long charging times and few charging stations makes them more vulnerable to conditions when energy consumption is higher than usual compared to vehicles driven by fossil fuel. This thesis focuses on vehicle and environment attributes that create energy-consuming forces resisting the vehicle motion, i.e. the *motion resistance* and how to model and estimate them.

The method developed in the thesis is based on a separation principle where attributes affecting the motion resistance are separated into vehicle, road and weather characteristics. This enables using vehicle data from heterogeneous vehicles to estimate local road weather conditions. The method is validated using simulations and real vehicle experiments.

The results show that the road and weather conditions can be estimated using data from connected vehicles and energy consumption of heavy-duty vehicle combinations is largely affected by crosswinds. Furthermore, the motion resistance from crosswinds can be characterized by simple models with only a few tuning parameters.

The main conclusions from this work are that road weather conditions including crosswinds need to be accounted for in range estimation algorithms, road weather estimates based on connected vehicle data is a promising technique, and windy days need to be anticipated in advance to avoid potential charging chaos.

Keywords: Range estimation, motion resistance, state estimation, rolling resistance, air resistance, road vehicles, commercial heavy vehicle combinations, passenger cars.

List of Publications

This thesis is based on the following publications:

[A] **Mikael Askerdal, Jonas Fredriksson**, "Vehicle Independent Road Section Resistance Estimation". *Published in Proceedings of EVS30*, vol. 1, pp. 88–99, ©(2017) by The European Association for Electromobility (AVERE) ISBN: 978-1-5108-6370-5.

[B] **Mikael Askerdal, Jonas Fredriksson**, "Vehicle Independent Road Resistance Estimation Using Connected Vehicle Data". *Published in Proceedings of AVEC'18, 14th International Symposium on Advanced Vehicle Control, Beijing, July 16-20, 2018.*

[C] **Mikael Askerdal, Jonas Fredriksson and Leo Laine**, "A Comparison of Simplified Air Drag Models Including Crosswinds for Commercial Heavy Vehicle Combinations". *In review for Vehicle Systems Dynamics Journal, 2023.*

Acknowledgments

First, I would like to express my gratitude to my supervisor Prof. Jonas Fredriksson for his invaluable interest, feedback and engagement. You are also a good friend. Additionally, this work would not have been possible without the generous support from the Swedish Electromobility Centre, who financed parts of my research.

I am also grateful to Volvo, for the colleagues with your expertise and knowledge and for the tools and data provided. Special thanks to my former manager Nicolas Andersson and my industrial supervisor Prof. Leo Laine, without your support and energy my research would not have been restarted.

Lastly, I would like to thank my family and my friends, especially my children, my partner in life and her wonderful children. You truly are an inspiration to me and helps me keep my motivation high.

Contents

Part I

Overview

CHAPTER 1

Introduction

1.1 Background

One of the challenges yet to be solved for battery electric vehicles (BEV) is how to deal with the limitation in driving distance before a recharge is needed [1]. This combined with the limited number of public charging stations, and the relatively long battery charging time makes accurate range estimation essential for reducing range anxiety and earning the public's trust. In principle, range estimation is simple, calculate the vehicle power consumption on the presumed road and integrate this power until the resulting energy equals the remaining battery energy. However even though simple in principle, range estimation is a complex task that involves many uncertainties.

First of all, what route to take needs to be determined. This is dependent on the travel distance, the traffic situation and the charging station availability of each route. In a city environment, the number of feasible routes could be huge, it is hence desirable to find a fast method to estimate the vehicle energy consumption on each route. Once the route is known, vehicle range can be estimated on that particular route. With the route given, range estimation is about knowing how much energy is available and predicting how long that

energy will last. The next step is determining the energy conversion rate that depends on both auxiliary systems and propulsion. Propulsion energy conversion can be broken down further into dependency on the vehicle speed profile, powertrain efficiency and resistance forces. The vehicle speed profile is normally not well known and can vary a lot depending on both driver and the traffic conditions [2], [3]. The powertrain efficiency is dependent on the efficiencies of the powertrain components such as the battery, electric machine, transmission, etc., and how the powertrain is controlled.

Assuming that both the vehicle speed profile and the powertrain efficiency are well known, it is still difficult to accurately predict the propulsion energy consumption due to the variations in forces from the road and the environment that resists the vehicle motion. The sum of all these forces is what is called *motion resistance*[1] in this thesis. Motion resistance can be divided into three main components, rolling resistance, air drag and grade resistance and is dependent on the road itself, the weather and the vehicle. How it affects vehicle energy consumption can be derived from the standard equation for longitudinal vehicle dynamics (force balance),

$$ma_v = F_{prop} - \frac{\rho C_d A}{2} v_{ax}^2 - mgC_r \cos(\alpha) \ - mg\sin(\alpha), \tag{1.1}$$

where m is the vehicle mass, a_v the vehicle acceleration, F_{prop} the propulsion force, ρ the air density, C_d the air drag coefficient, A the frontal area, v_{ax} the longitudinal airspeed (i.e. the sum of vehicle speed and the headwind speed), g the gravitational constant, C_r the rolling resistance coefficient and α the longitudinal road gradient. Integrating the force balance, equation 1.1, over a road segment from start position 0 to end position S gives the corresponding energy balance equation:

$$m\frac{(v_v^2(S) - v_v^2(0))}{2} = W_{wheel} - \frac{\rho C_d A S}{2}\overline{v}_{ax}^2 - mgC_r S_h - mg(h_r(S) - h_r(0)) \tag{1.2}$$

where v_v is the vehicle speed, W_{wheel} the total wheel energy for the vehicle combination over the road segment, $\overline{v}_{ax}$ the root mean square of the longi-

[1] In the papers in part II of the thesis, the term *road resistance* is used frequently. It has the same meaning as motion resistance. The terminology was changed in order to avoid misunderstandings since the term road resistance sometimes is used for denoting rolling resistance as well.

tudinal airspeed on the road section, and $h_r(S)$ and $h_r(0)$ the altitude at position S and position 0 respectively. The motion resistance energy is the sum of the negative terms of the right side of equation 1.2, where $\frac{\rho C_d A S}{2}\overline{v}_{ax}^2$ is denoting the air drag energy, mgC_rS_h the rolling resistance energy and $mg(h_r(S) - h_r(0))$ the grade resistance energy. The relative importance of different motion resistance factors is presented in Appendix A.1. For the car, the relative sensitivity on air drag from headwind speed is roughly three times higher than the relative sensitivity from crosswind speed. For a rigid truck without a trailer, the relative importance is similar for the head- and crosswind speed while the relative sensitivity from crosswind speed is almost three times higher than the relative sensitivity from headwind speed on a tractor-semitrailer combination. The relative importance of different environmental factors is clearly not the same for all types of road vehicles.

Estimating motion resistance for road vehicles

Estimating motion resistance is difficult due to uncertainties in road and weather conditions as well as in the vehicle's parameters as seen in equation 1.2. For example, grade resistance is affected both by the road and the vehicle since road slope and vehicle mass interacts to create grade resistance. Air drag can be measured in a wind tunnel and air drag coefficients determined from those measurements. Still, if the exterior of the vehicle is modified in some way, for example by mounting a roof box on a car or attaching a trailer to a truck, the actual air drag coefficient can be very different from the calculated value from the wind tunnel tests. Energy losses due to rolling resistance come from the complex interaction between the road surface and the vehicle. Rolling resistance can be measured in rigs and a rolling resistance coefficient can be computed from these measurements. However, that coefficient is not generally applicable. If the tires or the operation conditions, like the weather, are changed so will the rolling resistance coefficient. How to model rolling resistance so that rolling resistance can accurately be computed for different combinations of vehicles in different driving and road weather conditions is still an open research question, [4], [5].

Road weather can be divided into ambient conditions, wind conditions and road surface conditions (here referring to the road weather aspects like dry or humid surface, amount of water or snow on the road, and road surface temperature). Road weather estimation is, a bit surprising considering the

vast amount of research papers dealing with range estimation, e.g. [6]–[8], sort of a white spot when it comes to research. Air drag and rolling resistance estimation have been investigated in several papers, e.g. [9]–[11], but it is often the estimation of the total effect from the resistances or the estimation in specific conditions, i.e. no wind (or at least no crosswinds) and dry asphalt road, rather than estimation of the road weather itself separated from the vehicle attributes that is investigated. This might partly be explained by difficulties in exciting the system enough to be able to do a separation into several different quantities, partly by difficulties in accurately measuring the road section wind speed and perhaps by an assumption that the effect of energy consumption from the wind on average is zero. It should be noted though that the separation may only be meaningful for applications that both can access road weather information and benefit from it. For example, for an algorithm that uses data of the anticipated weather conditions on the chosen route to calculate the remaining vehicle range, this separation is vital, while if such information is not available or if the interest is only to estimate the total instantaneous effect from the motion resistance, estimation of lumped parameters/effects may work equally good or better.

Ambient conditions are including air density, air temperature, sun intensity and precipitation. Air density has a direct effect on air drag (as seen in equation 1.2). Air temperature has an indirect effect on motion resistance since it is affecting both air density [12] and rolling resistance through the tire temperature [13]. Sun intensity is indirectly affecting the rolling resistance through heating and drying of the road surface and heating the tires. Precipitation is indirectly affecting rolling resistance through water and snow build-up on the road surface and cooling of both tires and road surface [14]. It also has a minor effect on air drag due to changes in vehicle surface roughness and acceleration of raindrops [15].

Wind conditions in the form of headwind speed have a direct effect on air drag as can be seen in equation 1.1, since the airspeed depends on both the vehicle's speed and the wind speed $v_{ax} = v_v + v_{wx}$. [16] also reports that, *"Adverse wind effect occurs for substantially more than half the possible wind angles relative to the road"*, which suggests that there is also a hidden indirect effect from crosswinds.

There are several different indirect effects on rolling resistance from road surface conditions. For example, [14] gives an overview of research papers

on how different road conditions affect rolling resistance for different types of vehicles. Poor road conditions, like a snowy road, can have at least as high influence on energy consumption as strong wind. From this, it can be concluded that road weather really does have a strong influence on vehicle energy conversion losses.

1.2 Problem Statement

The problem to be addressed through this thesis is the error in vehicle range estimation that is inflicted by prevailing road weather conditions. Remaining vehicle range estimation is crucial for BEVs due to the combination of the limited number of charging stations, long charging times and the limited amount of energy they carry. The energy consumption rate is affected by motion resistance which in turn is highly dependent on the road weather and road surface conditions [14], [17]. Strong winds and water or snow on the road are examples of known factors limiting the vehicle range [14], [18], [19]. This in combination with uncertainties in vehicle attributes and actual road weather conditions creates errors in vehicle range estimation.

Failing in taking road weather properly into account when doing range estimation may in the worst-case scenario cause an unwanted stop for a BEV where charging possibilities may be limited. Even if there is a charging station available, an unplanned stop for charging may be required resulting in a time loss that may be very costly for a time-critical mission. On a fleet level, this problem becomes even more severe since bad weather conditions tend to affect all vehicles in the same region at the same time potentially resulting in charging chaos unless carefully planned for.

To be able to estimate the influence on motion resistance from weather conditions, the road weather attributes and vehicle attributes impacting motion resistance need to be identified and estimated. Wind conditions at road level, road surface temperature, and water and snow levels on the road are all examples of relevant road weather data that are difficult to access for a complete route. Also, crosswinds' effects on air drag after an exterior change in a vehicle and how tire temperatures can be modeled in different road weather conditions are examples of important factors affecting motion resistance that may need to be investigated further.

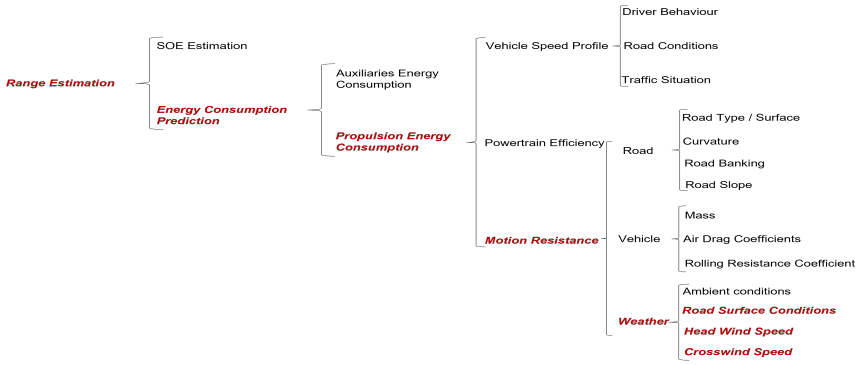

Figure 1.1: Range estimation overview

1.3 Limitations

Range estimation is a wide area and it is difficult to focus on everything at once and therefore this thesis is limited to effects from motion resistance in general and the effects affected by road weather in particular. The items in scope for this thesis have been highlighted with ***red, bold, italic text*** in Figure 1.1.

Battery State-Of-Energy (SOE) estimation, which is another topic for a vast amount of research [20]–[23] is out of scope for this thesis since it is not related to motion resistance. The same goes for the auxiliary systems' impact. They are for sure affected by weather but are not part of the motion resistance and are very much dependent on the application and hence difficult to treat in a general framework.

When it comes to powertrain efficiency, it is depending on both powertrain components and the energy management system. To be able to deal with that, detailed information about the system is needed. Since high powertrain efficiency contributes very much to the competitiveness of a vehicle, the development of efficient powertrains are left to the OEMs (original equipment manufacturer, i.e. the car (truck) maker) to do.

Research around driver modeling [24], [25], automated longitudinal control [26], [27], vehicle speed prediction and optimization in traffic [28]–[30], are all examples of research dealing with the vehicle speed profile. Apart from being already investigated, there is an additional reason for keeping the vehicle

speed profile out of the scope; it can to some extent be controlled by the driver or by an intelligent cruise controller. Hence, if a simple method to calculate the impact on energy consumption from different vehicle speed profiles is developed, the vehicle speed profile can be tailored to optimize the energy consumption or, even better, to optimize the overall transport mission target.

Road attributes are in general either more or less stationary over time, such as the curvature, road banking and road slope, or changing very slowly as the road surface. They can hence be measured once (in the former case) or with rather long intervals (as in the latter case) and stored in a database. The Swedish National Road and Transport Research Institute (VTI) has done so and stored measurements in a public database, *Long Term Pavement Performance*, [31]. Road slope as well as other road attributes can also be found in several maps services e.g. [32], [33]. Road attributes are therefore considered to be possible to find using known methods and are out of the scope of this research.

The same goes for some of the ambient conditions such as temperature, pressure and density. Many vehicles measure at least ambient temperature and pressure using standard sensors and some vehicles also measure ambient humidity. Using data from these sensors is considered to be enough to be able to compute for example a reasonably accurate air density estimate [12].

Precipitation is omitted due to lack of data. Results from [15] show that rain may have a significant impact on the air drag coefficient though. Also, when turning the attention to rolling resistance, the effects from ambient conditions such as precipitation and sun intensity are likely to be considered through their indirect effect on the road surface conditions.

Estimation of relevant vehicle parameters describing how sensitive the motion resistance is to different kinds of environmental factors is out of the scope of this thesis and they are instead assumed to be known. This is of course not always the case and it would for sure be interesting to investigate how vehicle parameters' estimates can be improved using road weather information going forward.

The scope of this thesis is also limited to simplified models with a limited number of parameters. The underlying motivation for this is that the intended usage of the developed models is range estimation which is a complex function including many different factors. If each of these factors is to be modeled in detail, the computational power needed is likely to be vast. The intention is

to produce models that are computationally light so that energy consumption for different routes with different vehicle speed profiles can be computed fast. For example, this rules out using Computational Fluid Dynamics (CFD) as a method for modeling air drag.

1.4 Thesis focus and contributions

The focus of this thesis is to investigate how road weather affects propulsion energy consumption and how road weather conditions can be estimated.

The idea utilized in this thesis is that of using data from connected vehicles running on the same road segment at roughly the same time to estimate road weather conditions. The initially developed road weather estimation algorithm was based on eight assumptions stated in Paper A, one being that there is no effect from side wind (crosswinds). It is shown that under these assumptions, the defined road weather conditions' parameters; the rolling resistance coefficient and the headwind speed, can analytically be calculated from the connected vehicle data. In Paper B this estimation method was validated through real vehicle tests. However, it shows that the assumption of no effect from crosswinds is far from true. Without the influence of crosswinds, the conclusion is that the method seems to work well though and is capable of picking up changes in both headwind speed as well as road surface conditions.

Paper C complements Paper A and B with the development of simplified air drag models that include the effect of crosswinds. In Chapter 2 it is shown how a model from Paper C can be incorporated and used in a road weather estimation algorithm using vehicle energy consumption data from heterogenous vehicles as input.

The main findings presented in this thesis are:

- In absence of crosswinds and if road surface conditions are the same in both driving directions, headwind speed and road surface conditions can be estimated from connected vehicle data using an analytical approach.
- Crosswinds have a significant effect on air drag and therefore also on vehicle energy consumption.
- An air drag model including only two or three parameters can describe the influence from crosswinds with fairly good accuracy.

1.5 Thesis outline

The thesis is divided into two main parts where the first part gives the context and application of the findings in the scientific papers appended in the second part. Chapter 2 shortly describes the modeling and estimation methods developed in appended papers in part II and results from those papers are presented in Chapter 3. Chapter 4 shortly summarizes the appended papers and Chapter 5 discusses and concludes the results and provides ideas for future work.

1.6 Notation

The following notation has been used all through part I of the thesis.

Symbol	Explanation
A	frontal area
A_p	frontal area projection
a_v	vehicle acceleration
α	longitudinal road gradient
α_p	vehicle energy consumption parameter
β	vehicle energy consumption parameter
C_d	air drag coefficient
C_r	rolling resistance coefficient
C_dA	product of air drag coefficient and frontal area projection
c_1	(nominal) air drag coefficient
c_2	(cross sensitive) air drag coefficient
c_3	(direct crosswind) air drag coefficient
$c_{r_{nom}}$	rolling resistance coefficient in nominal conditions
$c_{r_{road}}$	rolling resistance road condition coefficient
γ	vehicle energy consumption parameter
g	gravitational constant
h_r	altitude
i	vehicle index in forward direction
j	vehicle index in backward direction
m	vehicle mass
N_1	number of vehicles in forward direction

N_2	number of vehicles in backward direction
ρ	air density
S	road segment length
S_h	road segment horizontal length
t	time
θ	air attack angle
v_{ax}	longitudinal air speed
$\overline{v}_{ax}$	root mean square of the longitudinal air speed
v_v	vehicle speed
v_{wx}	longitudinal (or head) wind speed
v_{wy}	lateral (or cross-) wind speed
$\lvert\overline{v}_{wy}\rvert$	root mean square of lateral wind speed
$\overline{v}_{wy}^2$	mean square of lateral wind speed
$W_{roll-air}$	calculated sum of rolling resistance and air resistance energy
W_{wheel}	total wheel energy

Table 1.1: Notation.

CHAPTER 2

Methodology

This chapter is summarizing the method for estimating road weather conditions presented in the attached papers Paper A and Paper B. A further development including effects from crosswinds using a simplified air drag model from Paper C is also presented.

2.1 Road weather estimation

The wheel energy consumption model used is based on the standard equation for longitudinal vehicle dynamics (force balance), i.e. equation 1.1 and the energy balance equation given in equation 1.2. The basic idea is to divide a road into segments and let the vehicles passing each segment measure their energy consumption. This data can then be used to estimate the prevailing road weather on the road segments. The idea is illustrated in Figure 2.1. The yellow lines mark the start and the end of a road segment. The vehicles in the figure can be divided into three groups:

1. vehicles running on the road segment, illustrated by the truck,
2. vehicles that have passed the road segment, illustrated by the bus, and

3. vehicles that will pass through the road segment, illustrated by the two cars.

While running on the segment, the truck is measuring its energy consumption. The bus that has passed the segment subtracts the weather-independent wheel energy consumption, i.e., the change in potential and kinetic energy that has occurred over the segment, from the measured wheel energy and sends this information to a cloud-based parameter estimation algorithm. That information is complemented with data describing how sensitive that particular vehicle is to different kinds of road weather effects like headwinds, crosswinds and road surface conditions. The estimation algorithm uses this information to improve the estimates of the prevailing road segment weather conditions and sends it to the two cars that will pass the road segment. The cars can then use the updated road segment weather information to make a more accurate range prediction.

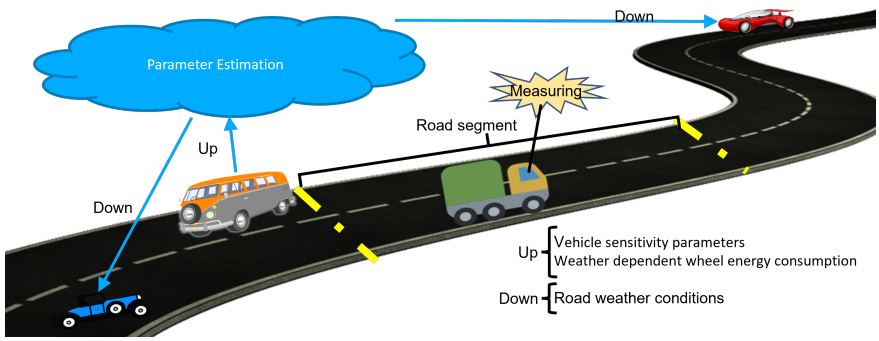

Figure 2.1: Road weather estimation using heterogeneous vehicles as measurement probes.

More formally, the energy at the wheels that a vehicle i has consumed for driving the segment is measured in the vehicle and denoted $W_{wheel,i}$. Subtracting the kinetic and potential energy from $W_{wheel,i}$ gives the i:th vehicle's weather-dependent wheel energy consumption. This is the sum of the rolling resistance and air resistance energy, $W_{roll-air,i}$:

$$W_{roll-air,i} = W_{wheel,i} - m_i g \left(h_r\left(S\right) - h_r\left(0\right)\right) - m_i \frac{\left(v_{v,i}^2\left(S\right) - v_{v,i}^2\left(0\right)\right)}{2}, \quad (2.1)$$

where m_i is the mass of the vehicle, and $v_{v,i}^2(S)$ and $v_{v,i}^2(0)$ the speed of the vehicle in point S and in point 0 respectively. $W_{roll-air,i}$ is the weather-dependent wheel energy consumption that is sent from the vehicle to the cloud-based parameter estimation algorithm. Now further assuming that crosswinds have an insignificant effect on energy consumption, the motion resistance can be determined as:

$$W_{roll-air,i} = \frac{\rho C_{d,i} A_i}{2} \int_0^S v_{ax,i}^2 ds + m_i g C_{r,i} S_h, \tag{2.2}$$

where S_h is the horizontal length of the road segment. If the head-wind speed, v_{wx} and the vehicle speed v_v are assumed to be independent, the integral of $v_{ax,i}^2$ becomes:

$$\int_0^S v_{ax,i}^2 ds = S(\overline{v}_{v,i} + \overline{v}_{wx})^2, \tag{2.3}$$

where $\overline{v}_{v,i}$ is the root mean square of the vehicle speed over the segment, and $\overline{v}_{wx}$ is the root mean square of the headwind speed. Now, $W_{roll-air,i}$ can be rewritten as:

$$W_{roll-air,i} = \frac{\rho C_{d,i} A_i S}{2} (\overline{v}_{v,i} + \overline{v}_{wx})^2 + m_i g C_{r,i} S_h. \tag{2.4}$$

By rearranging equation 2.4, completing the squares and normalize with vehicle mass, the normalized rolling resistance energy, $gC_{r,i}S_h$ can be written as:

$$gC_{r,i}S_h = \frac{W_{roll-air,i}}{m_i} - \frac{\rho C_{d,i} A_i S \overline{v}_{v,i}^2}{2m_i} - \frac{\rho C_{d,i} A_i S \overline{v}_{v,i}}{m_i} \overline{v}_{wx} - \frac{\rho C_{d,i} A_i S}{2m_i} \overline{v}_{wx}^2 \tag{2.5}$$

The normalized rolling resistance is in other words described by a second-order polynomial in wind speed and could be described as:

$$gC_{r,i}S_h = \alpha_{p,i} - \beta_i * \overline{v}_{wx} - \gamma_i * \overline{v}_{wx}^2 \tag{2.6}$$

where $\alpha_{p,i} = \frac{W_{roll-air,i}}{m_i} - \frac{\rho C_{d,i} A_i S \overline{v}_{v,i}^2}{2m_i}$, $\beta_i = \frac{\rho C_{d,i} A_i S \overline{v}_{v,i}}{m_i}$ and $\gamma_i = \frac{\rho C_{d,i} A_i S}{2m_i}$ are the parameters sent to the cloud algorithm (i.e. the blue cloud in Figure 2.1).

Now consider the case where N_1 vehicles are passing the same road segment in the same direction in a reasonable short time so that the wind and road surface can be considered to be constant over this period and that N_2 vehicles

are passing in the opposite direction in the same time period. If each of the vehicles contributes with the α_p, β and γ coefficients after running on the selected road segment, the collective sum of normalized rolling resistance becomes:

$$gS_h \sum_{i=1}^{N_1} C_{r,i} = \sum_{i=1}^{N_1} \alpha_{p,i} - \overline{v}_{wx} \sum_{i=1}^{N_1} \beta_i - \overline{v}_{wx}^2 \sum_{i=1}^{N_1} \gamma_i. \tag{2.7}$$

and

$$gS_h \sum_{j=1}^{N_2} C_{r,j} = \sum_{j=1}^{N_2} \alpha_{p,j} + \overline{v}_{wx} \sum_{j=1}^{N_2} \beta_j - \overline{v}_{wx}^2 \sum_{j=1}^{N_2} \gamma_j. \tag{2.8}$$

where i indicates data from vehicles traveling in one direction and j indicates data from vehicles traveling in the opposite direction.

If assuming that the mix of vehicles running in both directions are similar so that they on average have the same rolling resistance coefficient, the left-hand sides of equation (2.7) and equation (2.8) become equal if they are normalized with the respective number of vehicles that have passed in each direction, i.e. N_1 and N_2. Dividing equation (2.7) and (2.8) with N_1 and N_2 respectively, and putting them together gives:

$$\begin{aligned} &\frac{\sum_{i=1}^{N_1} \alpha_{p,i} - \overline{v}_{wx} \sum_{i=1}^{N_1} \beta_i - \overline{v}_{wx}^2 \sum_{i=1}^{N_1} \gamma_i}{N_1} = \\ &= \frac{\sum_{j=1}^{N_2} \alpha_{p,j} + \overline{v}_{wx} \sum_{j=1}^{N_2} \beta_j - \overline{v}_{wx}^2 \sum_{j=1}^{N_2} \gamma_j}{N_2} \end{aligned} \tag{2.9}$$

or

$$\begin{aligned} \overline{v}_{wx}^2 \left(\frac{\sum_{i=1}^{N_1} \gamma_i}{N_1} - \frac{\sum_{j=1}^{N_2} \gamma_j}{N_2}\right) + \overline{v}_{wx} \left(\frac{\sum_{i=1}^{N_1} \beta_i}{N_1} + \frac{\sum_{j=1}^{N_2} \beta_j}{N_2}\right) + \\ + \left(\frac{\sum_{j=1}^{N_2} \alpha_{p,j}}{N_2} - \frac{\sum_{i=1}^{N_1} \alpha_{p,i}}{N_1}\right) = 0. \end{aligned} \tag{2.10}$$

This is clearly a second-order equation in wind speed and can be solved analytically.

Once the wind speed is determined, the average C_r can be calculated using either equation (2.7), (2.8) or the sum of both. The latter holds information

from all vehicles and is therefore used in this thesis:

$$C_r = \frac{1}{2gS_h}\left(\frac{\sum_{i=1}^{N_1}\alpha_{p,i} - \overline{v}_{wx}\sum_{i=1}^{N_1}\beta_i - \overline{v}_{wx}^2\sum_{i=1}^{N_1}\gamma_i}{N_1} + \right. \\ \left. + \frac{\sum_{j=1}^{N_2}\alpha_{p,j} + \overline{v}_{wx}\sum_{j=1}^{N_2}\beta_j - \overline{v}_{wx}^2\sum_{j=1}^{N_2}\gamma_j}{N_2}\right). \tag{2.11}$$

The formulations in equation (2.1) and equation (2.2) are the basis of the framework for estimating wind speed and road surface conditions developed in Paper A and validated in Paper B.

Road weather estimation including crosswinds

The method presented in the previous section relies on several assumptions, one of them being that crosswinds either are not present or can be neglected. The validation through vehicle measurements in Paper B shows that the method works well when crosswind components are small but fails for higher crosswind speeds. Paper C investigates different simplified air drag models that include an explicit dependency on the crosswind speed which can be used in road weather estimation algorithms. Those models are based on some general definitions related to wind and airspeed. For a vehicle running with the speed v_v, the wind speed is divided into a headwind (longitudinal) speed component, v_{wx}, acting opposed to the vehicle's motion direction and a crosswind (lateral) component, v_{wy}, acting perpendicular to the vehicle motion direction, see Figure 2.2. The relative longitudinal airspeed then becomes the sum of the headwind speed and the vehicle speed, i.e.

$$v_{ax} = v_v + v_{wx} \tag{2.12}$$

while the relative lateral airspeed is the crosswind component v_{wy}. The total relative airspeed v_a can be determined from the two components as:

$$v_a = \sqrt{v_{ax}^2 + v_{wy}^2}, \tag{2.13}$$

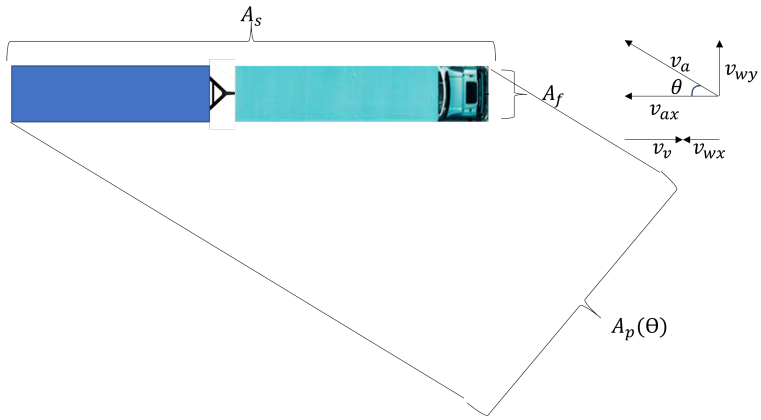

Figure 2.2: Definitions and notation of airspeeds, area projection, wind speeds and air attack angle.

and the angle between the total relative airspeed and the vehicle motion, commonly denoted as the so-called *air attack angle* becomes:

$$\theta = \arctan \frac{|v_{wy}|}{v_{ax}}. \tag{2.14}$$

Now using these definitions, equation 1.2 is still valid even in the presence of crosswinds if only letting $C_d A$ be dependent on θ. Paper C investigates simplified models for describing $C_d A(\theta)$. Those models can (with some minor adjustments [1]) all be written in either of two different forms,

$$C_d A(\theta) \approx \ (c_1 \cos^2(\theta) + c_2 \cos(\theta) sin(\theta) + c_3 \sin^2(\theta)) A_p(\theta), \tag{2.15a}$$

or,

$$C_d A(\theta) \approx \ (c_1 + c_2\theta) A_f \cos^2(\theta) + c_3 A_s \sin^2(\theta), \tag{2.15b}$$

where c_1, c_2 and c_3 are aerodynamic coefficients, $A_p(\theta)$ the area projection in the motion direction, A_f the frontal area and A_s the side area. If the air attack angle θ is 0, i.e. there are no crosswinds present, both variants

[1] For a full model of variant 2.15a where all three parameters c_1, c_2 and c_3 are used, it is argued in Paper C that the term $A_p(\theta)$ should be omitted. The change in area projection will instead appear in c_1, c_2 and c_3.

of equation 2.15 will collapse into the original model of equation 1.2. Now note that this approximation of C_dA is based on a convention that the square of the airspeed, v_a^2 is used for calculating the air drag. In the framework of Paper A and Paper B, the convention is to use the square of the longitudinal air speed, v_{ax}^2 instead. Therefore before the models of equation 2.15 can be used for the estimations, they need to be adjusted to the convention of using the longitudinal airspeed. By doing that, equation 2.15 becomes:

$$C_dA(\theta) \approx \ (c_1 + c_2 \tan(\theta) + c_3 \tan^2(\theta))A_p(\theta), \tag{2.16a}$$

or,

$$C_dA(\theta) \approx \ (c_1 + c_2\theta)A_f + c_3 A_s \tan^2(\theta). \tag{2.16b}$$

Now, using equation (2.16), equation (2.4) can be rewritten into

$$W_{roll-air,i} \approx \frac{\rho S}{2}(c_{1,i} + c_{2,i} \tan(\theta) + c_{3,i}\tan^2(\theta))A_p(\theta)\overline{v}_{ax,i}^2 + m_i g C_{r,i} S_h \tag{2.17a}$$

or

$$W_{roll-air,i} \approx \frac{\rho S}{2}((c_{1,i} + c_{2,i}\theta)A_f + c_{3,i}A_s\tan^2(\theta))\overline{v}_{ax,i}^2 + m_i g C_{r,i} S_h. \tag{2.17b}$$

As $\tan(\theta)\,\overline{v}_{ax,i} = \frac{|v_{wy}|}{\overline{v}_{ax,i}}\overline{v}_{ax,i} = |\overline{v}_{wy}|$, where $\overline{v}_{wy}$ is the crosswind speed, equation (2.17) can be simplified into

$$W_{roll-air,i} \approx \frac{\rho S}{2}(c_{1,i}\overline{v}_{ax,i}^2 + c_{2,i}|\overline{v}_{wy}|\overline{v}_{ax,i} + c_{3,i}\overline{v}_{wy}^2)A_p(\theta) + m_i g C_{r,i} S_h \tag{2.18a}$$

or

$$W_{roll-air,i} \approx \frac{\rho S}{2}((c_{1,i} + c_{2,i}\theta)A_f\overline{v}_{ax,i}^2 + c_{3,i}A_s\overline{v}_{wy}^2) + m_i g C_{r,i} S_h. \tag{2.18b}$$

Now even though equation 2.18 is in a similar format as equation 2.4, there is a fundamental difference. It now contains three unknown environmental parameters, i.e., $\overline{v}_{wx}$ (since $\overline{v}_{ax,i} = \overline{v}_{v,i} + \overline{v}_{wx}$), $\overline{v}_{wy}$ and $C_{r,i}$, instead of two. Since there are still only two measurement equations, one for each driving direction, c.f. equations 2.7 and 2.8, the analytical method will no longer work. Instead, it is recommended to use a standard state estimation method, for example, a Kalman Filter (KF) or Recursive Least Squares (RLS) for the

road weather estimation when crosswind speed is included.

CHAPTER 3

Results

The basic idea pursued for the estimation process in this thesis is to divide the effect of motion resistance into vehicle parameters, such as vehicle mass, aerodynamic coefficients, and tire coefficients and environmental parameters such as air density, wind speed, wind direction and road surface conditions that can be estimated in a cloud solution based on data from many vehicles running on the same road segment at approximately the same time.

The first section of this chapter presents some of the results from Paper A on road weather estimates from simulation data based on the assumption that crosswind has little or no effect on air drag. Then results of road weather estimates from vehicle measurements from Paper B are presented. The section thereafter presents different models from Paper C that can be used to include the effect from crosswinds before everything is put into context in the last section when the effect on vehicle energy consumption from different wind conditions is presented in a real-world example.

3.1 Estimation based on simulation data

In this section results from estimations using the analytical method presented in Paper A and summarized in Section 2.1 are presented. 27 different vehicles were simulated running in random order and random direction on a road segment. The data from these vehicles were then used as input to the estimation process that produced estimates of wind speed and average rolling resistance. Figure 3.1a shows the estimated wind speed against the total number of vehicles driven during constant conditions in both directions. The estimated wind speed converges to a somewhat higher wind speed than the actual wind speed. The reason is that in this estimation, the average vehicle speed over the segment has been used as $\overline{v}_v$ rather than the root mean square of the vehicle speed and this produces a bias in the wind speed estimate.

Figure 3.1b shows the corresponding estimated rolling resistance using the estimated wind speeds, as shown in Figure 3.1a. Note that the estimation seems to converge to a value very close to the actual average rolling resistance. The wind speed estimation is more sensitive to the errors in the constant speed assumption than the rolling resistance coefficient. Note also that as soon as at least one vehicle has been driven in each direction, the estimated average rolling resistance coefficient will be equal in both directions. This follows directly from the assumption that the average rolling resistance is equal in both directions.

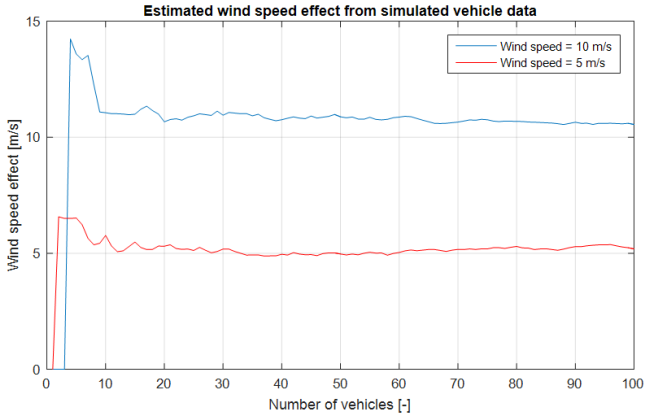

(a) Headwind speed estimation

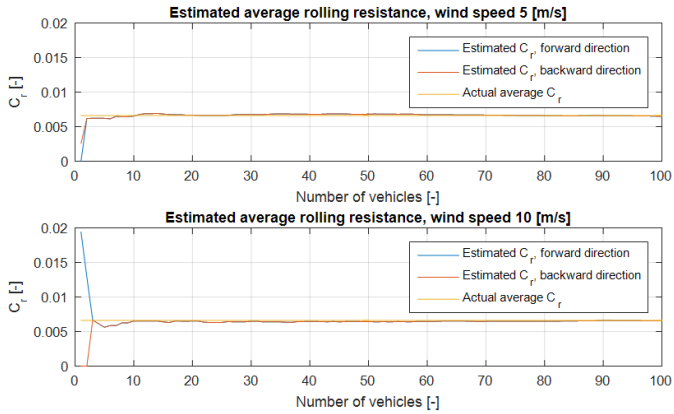

(b) Road surface estimation

Figure 3.1: Road weather estimation from multiple vehicles

3.2 Estimation based on measurements

To validate the estimation method, real vehicle measurements were conducted on a public road segment located south of Gothenburg, Sweden, with a truck equipped with a wind sensor that is able to measure the relative air speed and air direction. The road segment is 2060 meters long including both a

downhill and an uphill. The measurements were collected by running this road segment several times in both directions. Table 3.1 summarizes the measured average wind speed, average wind direction and road surface conditions during the measurements. Figure 3.2 illustrates the truck traveling in the forward

Date	Wind speed	Wind direction	Surface
2017-11-23	*2.7*	100°	Dry
2017-12-20	*1.8*	158°	Moist
2018-05-04	*2.0*	194°	Dry
2018-05-08	*1.4*	101°	Dry

Table 3.1: Road and Weather Measurements

direction with average wind speeds and wind directions during measurements marked. 0° means tailwind (in forward direction) and 180° means headwind.

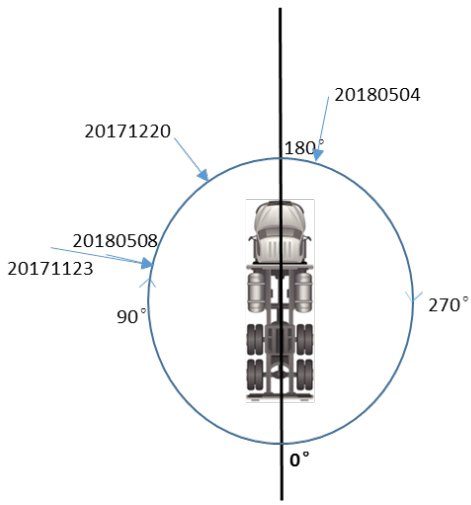

Figure 3.2: Average wind speed and wind direction during measurements

The reported wind speed from SMHI (Swedish Meteorological and Hydrological Institute) at the time and location for the measurements was between 4 and 9 m/s and the wind direction was either head or side wind (or a combination). However, the measured wind speed was much lower, < 3 m/s.

Table 3.2 presents the estimation results. As can be seen in Table 3.2, when there is a significant crosswind component, the estimated wind speed is neither close to the measured wind speed, nor the measured headwind speed vector component. Clearly, the crosswind speeds disturb the analytical estimation method.

Date	Measured wind speed	Estimated wind speed	Measured headwind speed vector component
2017-11-23	*2.7*	1.4	0.5
2017-12-20	*1.8*	2.0	1.7
2018-05-04	*2.0*	1.9	2.0
2018-05-08	*1.4*	0.6	0.3

Table 3.2: Measured and Estimated Wind Speed

3.3 Air drag models including crosswinds

The results in the last section suggest that the crosswind needs to be accounted for when estimating motion resistance. Simplified air drag models that include the crosswinds are addressed in Paper C and some of the results are summarized here.

The common way to include crosswind dependency in the air drag equation is to let the product of the air drag coefficient C_d and the frontal area A be a function of the air attack angle θ, i.e. $C_dA(\theta)$. Even though $C_dA(\theta)$ for a specific vehicle combination can be found with good accuracy from CFD calculations and wind tunnel tests, the result is in a tabulated form that complicates the wind conditions estimation process. Paper C investigates ways to get around this problem by representing $C_dA(\theta)$ with simplified analytical functions that have explicit dependencies on the wind conditions.

A requirement of the developed models is that the models should contain as few tuning parameters as possible. The reason for this is that the air drag properties change when the exterior of a vehicle combination changes. Air drag properties described by only a few tuning parameters enable online estimation of these parameters. Table 3.3 summarizes the model structures of $C_dA(\theta)$ developed in Paper C and Figure 3.3 compares these models with CFD data for three vehicle combinations for which the simplified models were

tuned to imitate. Model parameters, c_i, are found using least squares. Note that the $C_dA(\theta)$ values of the timber truck have been down-scaled by a factor of two in order to give it a similar magnitude as the other vehicle combinations and that the plotted $C_dA(\theta)$ are all values relative $C_dA(0)$ for the tractor with semitrailer combination. From a visual inspection, all models seem to perform reasonably well.

Table 3.3: Model structure overview.

Model	$C_dA(\theta)$
1	$c_1 \cos^2(\theta) A_p(\theta)$
2	$(c_1 \cos^2(\theta) + c_2 \cos(\theta)\sin(\theta)) A_p(\theta)$
3	$(c_1 A_f + c_2 A_s \theta)\cos^2(\theta)$
4	$(c_1 A_f + c_2 A_s \theta)\cos^2(\theta) + c_3 A_s \sin^2(\theta)$
5	$c_1 A_f \cos^2(\theta) + c_2 \sqrt{A_f A_s}\cos(\theta)\sin(\theta) + c_3 A_s \sin^2(\theta)$
6	$(c_1 + c_2 \sin(3\theta)) A_f$

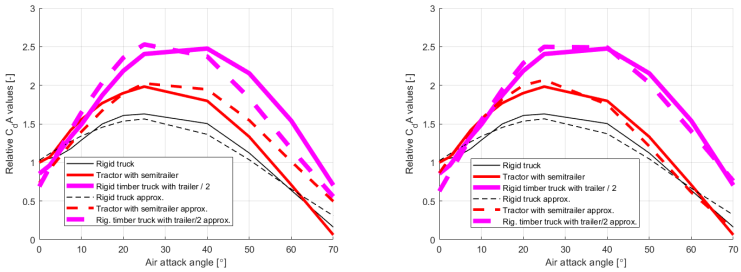

(a) Model 1 **(b)** Model 2

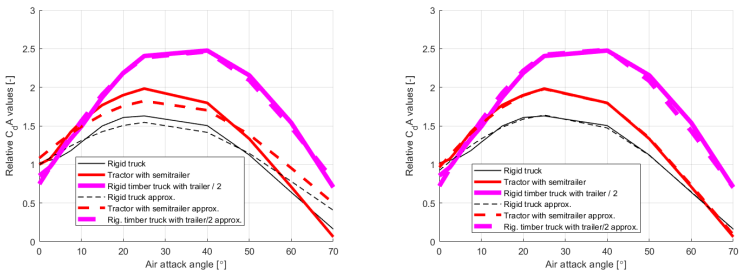

(c) Model 3 **(d)** Model 4

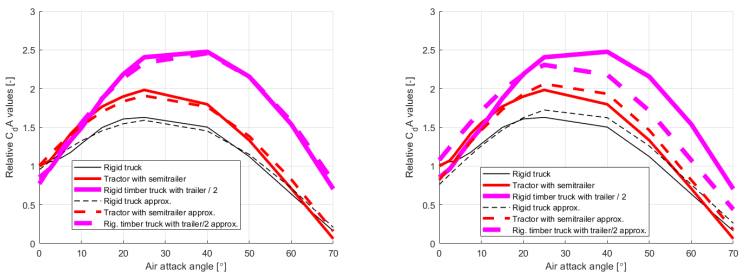

(e) Model 5 **(f)** Model 6

Figure 3.3: $C_dA(\theta)$ approximations as function of air attack angle θ for different types of vehicle combinations and model structures.

Table 3.4 compares the developed models using Root Mean Square (RMS) error as objective criteria. As a comparison Model 0 represents C_dA, i.e.

only the headwind component. As expected the models with more tuning parameters show better accuracy.

Table 3.4: RMS error for model fit.

Model	0	1	2	3	4	5	6
Rigid truck	2.55	0.58	0.57	0.65	**0.19**	0.26	0.60
Tractor/Semitrailer	3.23	1.19	0.51	1.04	**0.14**	0.38	0.51
Timber	6.83	1.71	1.18	0.79	0.64	**0.53**	2.58

3.4 Motion resistance effects on vehicle range

To illustrate the effect of the headwind and crosswind on vehicle energy and range estimation, a simple example is used. Consider a 34 tonnes tractor-semitrailer combination running on the well-known ACEA long-haul cycle promoted by the European Commission for CO_2 emission evaluation [34]. As the cycle starts and ends at the same altitude, the grade resistance energy is zero in the example. The analysis is done using the energy balance equation (1.2) and models presented in Paper C.

Figure 3.4 is showing how the energy at the driven wheels is distributed between braking, air drag and rolling resistance. The nominal air drag is the energy loss induced by the vehicle speed if no wind is present. The headwind drag shows how much extra energy that is lost if the cycle is run with a constant headwind component of 5 m/s. The crosswind drag is the additional drag loss if a crosswind component of 5 m/s is added to the no-wind conditions and the Head/Crosswind drag component is the additional drag losses from the interaction between the head- and the crosswind components that add upon the sum of the nominal and the individual head and crosswinds drag components. As a comparison, the maximum vehicle speed in the ACEA long-haul cycle is around 24 m/s, the average speed around 22 m/s and the minimum speed 0 m/s.

If effects from wind are neglected, then rolling resistance is the largest energy loss while if adding a 5 m/s headwind component, air drag and rolling resistance become similar in size. If also a crosswind component of the same magnitude is added, the total air drag becomes the largest energy loss by far.

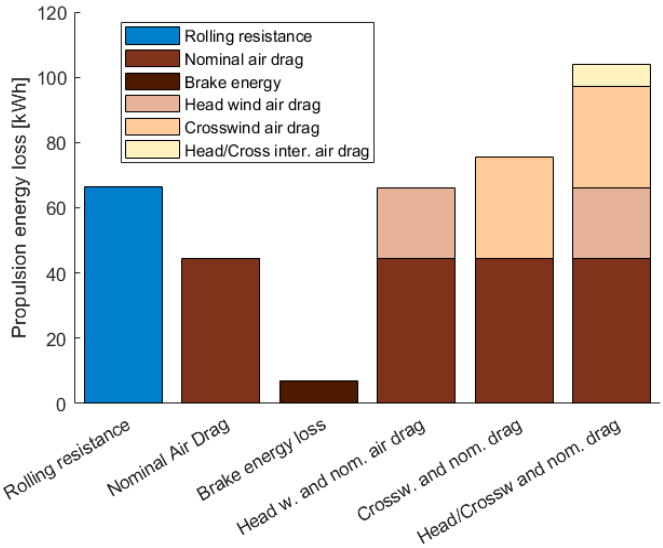

Figure 3.4: Energy loss distribution for 34 tonnes tractor with semitrailer on the ACEA long-haul drive cycle.

For comparison, the energy loss when braking (assuming that 30 % of the total brake energy are losses in battery, transmission, electric machines and service brake usage when electric machine braking capability is not sufficient) is also illustrated.

To study the effect of road weather conditions in a more realistic scenario, an energy consumption analysis is performed on the road between Malmö and Göteborg. Hourly wind data from SMHI's weather stations at several different positions on the route, i.e. Malmö, Helsingborg, Ängelholm, Halmstad, and Göteborg, in the time frame from 2000-01-01 to 2022-03-01 together with vehicle data for three different vehicle types are used in this analysis. Air drag data for the given vehicle combinations are visualized in Figure 3.5. Data shows that the air drag energy consumption of the car is much less influenced by crosswinds than the two truck combinations. The vehicle speed has been assumed to be constant all the way from Malmö to Göteborg.

Figure 3.6 is illustrating the air drag energy loss distributions for the car, the rigid truck without a trailer and the tractor with a semitrailer combination.

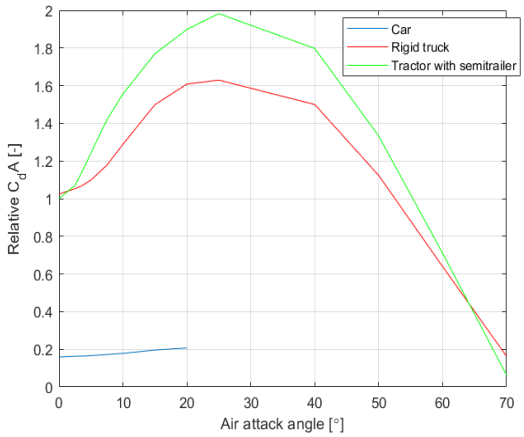

Figure 3.5: C_dA data

The figure shows the energy consumption distributions for running at nominal

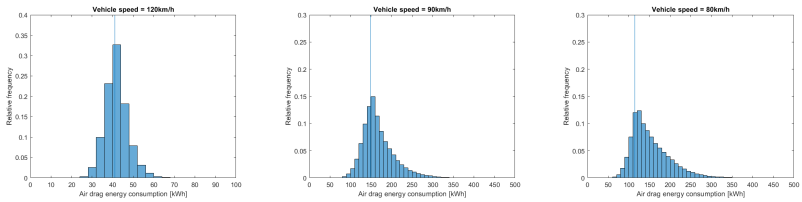

(a) Car, 120 km/h **(b)** Rigid truck, 90 km/h **(c)** Tractor - semitrailer, 80 km/h

Figure 3.6: Air drag energy consumption distributions for driving with constant speed between Malmö - Göteborg from 2000-01-01 to 2022-03-01

speeds for each combination (120 km/h for the car, 90 km/h for the rigid truck and 80 km/h for the tractor with semitrailer). The blue line shows the air drag energy consumption in nominal conditions which are defined as no wind and nominal vehicle speed. The air drag energy consumption spread grows with the size of the side area.

CHAPTER 4

Summary of included papers

This chapter provides a summary of the included papers.

4.1 Paper A

Mikael Askerdal, Jonas Fredriksson
Vehicle Independent Road Section Resistance Estimation
Published in Proceedings of EVS30, vol. 1, pp. 88–99, ©(2017) by The European Association for Electromobility (AVERE) ISBN: 978-1-5108-6370-5.

This paper addresses how to estimate motion (road) resistance parameters using vehicle log data. Motion resistance is commonly divided into three different components; rolling resistance, wind resistance and resistance from road gradient (hills). The total sum of motion resistance is the force that must be delivered by the powertrain to the wheels of the vehicle to maintain speed. The idea pursued in this paper is that it is possible to find models for each of the different components of the motion resistance where the input parameters used are separated into purely vehicle-dependent and purely vehicle-independent

parameters and that it is possible to estimate vehicle independent parameters from log data from a large population of vehicles (big data). The advantages of this approach are that data from any vehicle can be used to improve the estimation and that all vehicles can benefit from the estimated data. In the long run, this can lead to a system that dynamically calculates the surrounding parameters of the motion resistances and that adapts rapidly to changing conditions such as wind and wet road surface. The main benefit of using the results is improved range estimation of battery electric vehicles but it can also be used for less computational route planning and improved vehicle energy management. It is shown that road surface conditions and prevailing wind conditions can be determined only using vehicle log data if the effect from crosswinds is neglected.

4.2 Paper B

Mikael Askerdal, Jonas Fredriksson
Vehicle Independent Road Resistance Estimation Using Connected Vehicle Data
Published in Proceedings of AVEC'18, 14th International Symposium on Advanced Vehicle Control, Beijing, July 16-20, 2018.

This paper is investigating if it is possible to use vehicle log data to estimate vehicle independent motion (road) resistance parameters that can have large local variations and change rapidly, such as wind speed, wind direction and road surface conditions. The estimated parameters can be used to improve range estimation, route planning and vehicle energy management. The advantage with using vehicle independent parameters is that data from any vehicle can be used to improve the estimation and that all vehicles can benefit from the estimated data. An analytical solution previously presented for parameter estimation in Paper A is verified on vehicle log data. Results show that the method works reasonably well for wind speed estimation and that changes in road conditions can be detected. It is also pointed out that side wind affects need to be considered in future work. The sensitivity on vehicle energy consumption from errors in different road weather parameters is also investigated.

4.3 Paper C

Mikael Askerdal, Jonas Fredriksson and Leo Laine
A Comparison of Simplified Air Drag Models Including Crosswinds for Commercial Heavy Vehicle Combinations
In review for Vehicle Systems Dynamics Journal, 2023.

This paper addresses how to incorporate effects from crosswinds in a motion (road) resistance model similar to the model framework presented in Paper A and Paper B. Accurate range prediction requires good knowledge of the prevailing wind conditions and how they affect the energy consumption of the ego vehicle. A few different simplified vehicle air drag models that explicitly include the effect from crosswinds are presented and compared through some objective criteria. The models are developed from the normal air drag equation where the effect from wind is implicit and therefore often forgotten or neglected. The purpose is to find a low complexity model complementing CFD models and wind tunnel tests, that can be used for range estimation and predictive energy management algorithms. To simplify online estimation, a requirement is that the air drag models only contain a few tuning parameters. The models are validated against CFD calculations for a few vehicle combinations and the best models show good accuracy for air attack angles up to at least 60 degrees. It is shown that the parameters of the simplified models can loosely be connected to some basic geometrical attributes of a vehicle combination so it should be possible to give at least a rough estimate of the parameters of a simplified model based on these geometrical attributes. This is useful for making a first estimate of the aerodynamic properties of a vehicle combination after major changes in the exterior, e.g., when adding a trailer. It also highlights that the size and the shape of the vehicle side may be mainly responsible for the high longitudinal air drag sensitivity to crosswinds for large vehicle combinations.

CHAPTER 5

Concluding Remarks

Conclusions of the most important results are summarized in the section Conclusions followed by a discussion around the results and ideas of possible future research topics in the Discussion and future work section.

5.1 Conclusions

Connected vehicles is a promising technique for determining local weather conditions. The methods developed in this thesis are based on a separation principle where attributes affecting the motion resistance are separated into vehicle and road and weather characteristics. This enables using vehicle data from heterogeneous vehicles for estimating road and weather conditions. The method presented in this thesis has been validated using both simulation studies and real vehicle tests. The real experimental validations show that crosswind has a huge impact on the accuracy of the road and weather conditions estimation. The estimated conditions could be used by any vehicle for improving energy consumption predictions. Furthermore, road weather conditions need to be accounted for in range estimation algorithms as it has a considerable impact on energy consumption.

The thesis has also developed simplified air drag models including crosswinds suitable for use in energy consumption calculations. The models are verified using CFD calculations. The developed models can be used in range estimation algorithms and also included in the road weather estimations method presented.

5.2 Discussion and future work

The research behind this thesis started a few years back. At the time being, services using connected vehicle data were more or less non-existing but the development in this area has exploded since then, resulting in several services provided by companies such as HERE, Google, etc.

An advantage of using data from several vehicles for road weather conditions estimates compared to trying to do these estimates in a single vehicle is that the system can get excited from the differences in the vehicles and how they are affected by the road weather rather than from how the vehicle is driven. This enables individual estimation of road weather parameters, e.g. the wind speed, wind direction and road surface conditions even on flat road segments on which vehicles are keeping a constant speed. Hence the importance of getting data from *heterogeneous* vehicles.

By combining the idea of using connected vehicle measurements from Paper A with the air drag models of Paper C, it should be possible to estimate environmental characteristics. As mentioned in Section 2, the analytical method from Paper A will not work though since now there will be three unknown parameters to estimate, i.e. rolling resistance coefficient, headwind speed and crosswind speed, and only two equations, one for each driving direction. Instead standard estimation methods such as recursive least squares (RLS) or some kind of Kalman filter (KF) could be used. This is left as future work to show.

Another possible extension to this could be to complement the information from the connected vehicles with external information from weather institutes, and/or road weather measurement stations.

The air drag contribution to motion resistance is investigated in Paper C. Here examples of several different models are developed. It is interesting to see that simple models using only a few air drag coefficients seem to be capable of including the influence from crosswinds quite well. However, most of the

work presented in this thesis is based on data from simulations. To be really reliable, the developed models need to be validated. Collecting data from vehicle measurements and comparing the motion resistance calculated from those measurements with the developed models could be another topic for future research.

The relative importance of different environmental factors based on the models developed in paper C is presented in Appendix A.1. A still open research question is if the road weather effects on rolling resistance can be described using models of similar complexity as for the air drag. The importance of being able to predict the rolling resistance in different road surface conditions may increase in the future due to the anticipated more dramatic weather phenomena that follows upon climate change.

In a scenario with a high degree of electrification, the high wind sensitivity for large vehicle combinations that can be seen in Figure 3.6 may result in a dramatic increase in the number of vehicles require charging at the same time only due to the increase in air drag energy on windy days. If being able to predict this extra energy need in advance based on weather forecasts, the drivers and/or logistic companies can avoid the potential waiting time that follows from a deficit in charging opportunities by, for example, reducing the vehicle speed, rerouting to avoid the bad weather conditions altogether, reducing the payload, forming vehicle platoons, adding a temporary range extender on exposed vehicles or rescheduling the transport to another day. This underlines the importance of taking the weather effects into account already in the planning stages.

When looking at the air drag energy distributions in Figure 3.6 it should be noted though that the wind information is taken directly from the weather stations. That wind data represents the wind speeds ten meters up in the air. The wind speed at the vehicle level is most likely lower and hence, the variance in air drag conversion losses should in reality be a bit lower than the presented figures. However, it should also be noted that variance in air density and road surface conditions has been omitted. Adding the effect from the variances in those conditions would increase the energy consumption variance again to a level possibly close to or even higher than the presented.

Finally, with knowledge of what factors affect the spread of energy consumption and how they affect energy consumption together with an accurate road weather information source, each transportation company and/or driver

have the possibility to make accurate vehicle energy consumption predictions and take the necessary actions to minimize the impact of unfavorable energy consumption conditions. The available charging points can then be used by the vehicles with the dearest need. This may enable a sustainable transport solution that can be accepted both by the transportation companies as well as society.

References

[1] J. Dong, X. Wu, C. Liu, Z. Lin, and L. Hu, "The impact of reliable range estimation on battery electric vehicle feasibility," *International Journal of Sustainable Transportation*, vol. 14, no. 11, pp. 833–842, Sep. 2020, ISSN: 15568334.

[2] C. Fiori, V. Arcidiacono, G. Fontaras, *et al.*, "The effect of electrified mobility on the relationship between traffic conditions and energy consumption," *Transportation Research Part D: Transport and Environment*, vol. 67, pp. 275–290, Feb. 2019, ISSN: 13619209.

[3] S. Gupta, S. R. Deshpande, P. Tulpule, M. Canova, and G. Rizzoni, "An Enhanced Driver Model for Evaluating Fuel Economy on Real-World Routes," in *IFAC-PapersOnLine*, vol. 52, Elsevier B.V., 2019, pp. 574–579.

[4] H. Jansson and M. Åsenius, "The relation between rolling resistance and tyre temperature in real driving scenarios," Ph.D. dissertation, Linköping University, Linköping, Jun. 2021.

[5] L. Ydrefors, *The relationship between rolling resistance and tyre operating conditions, with a focus on tyre temperature*, ISBN: 9789180402668.

[6] H. Rahimi-Eichi and M. Y. Chow, "Big-data framework for electric vehicle range estimation," in *IECON Proceedings (Industrial Electronics Conference)*, Institute of Electrical and Electronics Engineers Inc., Feb. 2014, pp. 5628–5634, ISBN: 9781479940325.

[7] S. Sautermeister, M. Falk, B. Baker, F. Gauterin, and M. Vaillant, "Influence of measurement and prediction uncertainties on range estimation for electric vehicles," *IEEE Transactions on Intelligent Transportation Systems*, vol. 19, no. 8, pp. 2615–2626, Aug. 2018, ISSN: 15249050.

[8] Y. Zhang, W. Wang, Y. Kobayashi, and K. Shirai, "Remaining driving range estimation of electric vehicle," in *2012 IEEE International Electric Vehicle Conference, IEVC 2012*, 2012, ISBN: 9781467315623.

[9] R. Andersson, "Online Estimation of Rolling Resistance and Air Drag for Heavy Duty Vehicles," Ph.D. dissertation, KTH, Stockholm, 2012.

[10] H. S. Bae, J. Ryu, and J. C. Gerdes, "Road Grade and Vehicle Parameter Estimation for Longitudinal Control Using GPS," in *IEEE Intelligent Transportation Systems Conference Proceedings*, Oakland (CA), US, Aug. 2001, pp. 166–171.

[11] D. Zhang, A. Ivanco, and Z. Filipi, "Model-Based Estimation of Vehicle Aerodynamic Drag and Rolling Resistance," *SAE International Journal of Commercial Vehicles*, vol. 8, no. 2, pp. 433–439, Sep. 2015, ISSN: 19463928.

[12] F. E. Jones, "The Air Density Equation and the Transfer of the Mass Unit," Tech. Rep. 5.

[13] S. K. Srirangam, K. Anupam, C. Kasbergen, A. Scarpas, and V. Cerezo, "Study of Influence of Operating Parameters on Braking Friction and Rolling Resistance," *Transportation Research Record: Journal of the Transportation Research Board*, vol. 2525, no. 1, pp. 79–90, Jan. 2015, ISSN: 0361-1981.

[14] A. Carlson and T. Vieira, "The effect of water and snow on the road surface on rolling resistance," Tech. Rep.

[15] H. Fatahian, H. Salarian, M. Eshagh Nimvari, and J. Khaleghinia, "Numerical simulation of the effect of rain on aerodynamic performance and aeroacoustic mechanism of an airfoil via a two-phase flow approach," *SN Applied Sciences*, vol. 2, no. 5, May 2020, ISSN: 25233971.

[16] G. Sovran, "The Effect of Ambient Wind on a Road Vehicle's Aerodynamic Work Requirement and Fuel Consumption," Tech. Rep., 1984, pp. 449–472. [Online]. Available: `https://about.jstor.org/terms`.

[17] J. Wang, I. Besselink, and H. Nijmeijer, "Electric vehicle energy consumption modelling and prediction based on road information," *World Electric Vehicle Journa*, vol. 7, no. 3, pp. 447–458, Sep. 2017.

[18] Z. Yi and P. H. Bauer, "Sensitivity Analysis of Environmental Factors for Electric Vehicles Energy Consumption," in *2015 IEEE Vehicle Power and Propulsion Conference, VPPC 2015 - Proceedings*, Institute of Electrical and Electronics Engineers Inc., Dec. 2015, ISBN: 9781467376372.

[19] Smuts Martin, Scholtz Brenda, and Wesson Janet, "A Critical Review of Factors Influencing the Remaining Driving Range of Electric Vehicles," in *1st International Conference on Next Generation Computing Applications (NextComp)*, 2017, pp. 196–201, ISBN: 9781538638316.

[20] Q. Wang, J. Wang, P. Zhao, J. Kang, F. Yan, and C. Du, "Correlation between the model accuracy and model-based SOC estimation," *Electrochimica Acta*, vol. 228, pp. 146–159, Feb. 2017, ISSN: 00134686.

[21] J. Meng, M. Ricco, G. Luo, *et al.*, "An Overview and Comparison of Online Implementable SOC Estimation Methods for Lithium-Ion Battery," *IEEE Transactions on Industry Applications*, vol. 54, no. 2, pp. 1583–1591, Jan. 2018, ISSN: 00939994.

[22] J. Lee, O. Nam, and B. H. Cho, "Li-ion battery SOC estimation method based on the reduced order extended Kalman filtering," *Journal of Power Sources*, vol. 174, no. 1, pp. 9–15, Nov. 2007, ISSN: 03787753.

[23] J. P. Rivera-Barrera, N. Muñoz-Galeano, and H. O. Sarmiento-Maldonado, *Soc estimation for lithium-ion batteries: Review and future challenges*, Dec. 2017.

[24] A. Y. Ungoren and H. Peng, "An adaptive lateral preview driver model," *Vehicle System Dynamics*, vol. 43, no. 4, pp. 245–259, Apr. 2005, ISSN: 00423114.

[25] S. Kharrazi, M. Almen, E. Frisk, and L. Nielsen, "Extending behavioral models to generate mission-based driving cycles for data-driven vehicle development," *IEEE Transactions on Vehicular Technology*, vol. 68, no. 2, pp. 1222–1230, Feb. 2019, ISSN: 00189545.

[26] C. Lu, J. Dong, and L. Hu, "Energy-Efficient Adaptive Cruise Control for Electric Connected and Autonomous Vehicles," *IEEE Intelligent Transportation Systems Magazine*, vol. 11, no. 3, pp. 42–55, Sep. 2019, ISSN: 19411197.

[27] C. Huang, R. Salehi, and A. G. Stefanopoulou, "Intelligent Cruise Control of Diesel Powered Vehicles Addressing the Fuel Consumption Versus Emissions Trade-off," in *Annual American Control Conference (ACC)*, 2018, pp. 840–845, ISBN: 9781538654279.

[28] S. Lefèvre, C. Sun, R. Bajcsy, and C. Laugier, "Comparison of parametric and non-parametric approaches for vehicle speed prediction," in *Proceedings of the American Control Conference*, Institute of Electrical and Electronics Engineers Inc., 2014, pp. 3494–3499, ISBN: 9781479932726.

[29] J. Shin and M. Sunwoo, "Vehicle Speed Prediction Using a Markov Chain with Speed Constraints," *IEEE Transactions on Intelligent Transportation Systems*, vol. 20, no. 9, pp. 3201–3211, 2019, ISSN: 15580016.

[30] M. Yan, M. Li, H. He, and J. Peng, "Deep learning for vehicle speed prediction," in *Energy Procedia*, vol. 152, Elsevier Ltd, 2018, pp. 618–623.

[31] VTI, *Long Term Pavement Performance DataBase*, 2022. [Online]. Available: `https://www.vti.se/tjanster/vag--och-geoteknik/ltpp-databas`.

[32] HERE, *HERE maps elevation profile*, May 2022. [Online]. Available: `https://developer.here.com/documentation/routing-api/dev_guide/topics/use-cases/elevation-profile.html`.

[33] A. Schneider, *GPS Visualizer*, May 2022. [Online]. Available: `https://www.gpsvisualizer.com/`.

[34] European Commision, *Vehicle Energy Consumption calculation TOol – VECTO*. [Online]. Available: `https://ec.europa.eu/clima/eu-action/transport-emissions/road-transport-reducing-co2-emissions-vehicles/vehicle-energy-consumption-calculation-tool-vecto_en#ecl-inpage-537`..

APPENDIX A

Appendix

A.1 Sensitivity analysis

In this appendix, how sensitive the energy loss calculations are to accuracy in vehicle and road weather parameters is analyzed.

Vehicle energy conversion losses sensitivity on road weather and vehicle parameters

Both vehicle characteristics as well as road weather have a strong impact on the vehicle energy conversion losses such as rolling resistance and air drag. Here, the loss sensitivity for different parameters are investigated and compared.

From equations 1.2 and 2.18a, $W_{wheel}(i)$ can be approximated to

$$W_{wheel}(i) \approx$$
$$\approx \frac{\rho S(i)}{2}(c_1\overline{v}_{ax}^2(i) + c_2|\overline{v}_{wy}(i)|\overline{v}_{ax}(i) + c_3\overline{v}_{wy}^2(i)) + mgc_{r_{nom}}\overline{c}_{r_{road}}(i)S_h(i) +$$
$$+mg(h_r(d_e(i)) - h_r(d_0(i))) + m\frac{(v_v^2(d_e(i)) - v_v^2(d_0(i)))}{2}, \tag{A.1}$$

where $S(i)$ is the length of road segment i, $S_h(i)$ the horizontal length of road segment i, $\overline{x}$ denotes the root mean square of variable x over the road segment and $d_e(i)$ and $d_0(i)$ being the road segment end and start positions respectively. The rolling resistance coefficient, C_r has been divided into the product of a tire-dependent factor, $c_{r_{nom}}$, and a road surface dependent factor $c_{r_{road}}$ to complete the separation between vehicle and environment parameters. In equation A.1 there are both vehicle parameters and environmental parameters that need to be estimated. Some of them are easier to estimate than others. This section evaluates how sensitive the energy conversion losses at the wheels are to changes in different parameters. The purpose of this is to highlight what parameters that require good accuracy in their estimates and which that do not have such high requirements.

By differentiating equation A.1 with respect to each parameter, the overall sensitivity for errors in each parameter that needs estimation can be calculated. The sensitivity for errors in the vehicle parameters become

$$\frac{\partial W_{wheel}}{\partial c_1} = \frac{\rho S}{2}\overline{v}_{ax}^2 \qquad [\frac{J}{m^2}], \tag{A.2}$$

$$\frac{\partial W_{wheel}}{\partial c_2} = \frac{\rho S}{2}|\overline{v}_{wy}|\overline{v}_{ax} \qquad [\frac{J}{m^2}], \tag{A.3}$$

$$\frac{\partial W_{wheel}}{\partial c_3} = \frac{\rho S}{2}\overline{v}_{wy}^2 \qquad [\frac{J}{m^2}], \tag{A.4}$$

$$\frac{\partial W_{wheel}}{\partial m} = g\left(c_{r_{nom}}c_{r_{road}}S_h + h_r\left(S\right) - h_r\left(0\right)\right) \qquad [\frac{J}{kg}], \tag{A.5}$$

$$\frac{\partial W_{wheel}}{\partial c_{r_{nom}}} = mgc_{r_{road}}S_h \qquad [\frac{N}{-}]. \tag{A.6}$$

The sensitivity for errors in the road weather parameters become

$$\frac{\partial W_{wheel}}{\partial \overline{v}_{wx}} = \frac{\partial W_{wheel}}{\partial \overline{v}_{ax}} \frac{\partial \overline{v}_{ax}}{\partial \overline{v}_{wx}} = \rho S \left(c_1 \overline{v}_{ax} + \frac{c_2 |\overline{v}_{wy}|}{2} \right) * D \qquad [\frac{J}{m/s}], \text{ (A.7)}$$

$$\frac{\partial W_{wheel}}{\partial \overline{v}_{wy}} = \rho S \left(c_3 |\overline{v}_{wy}| + \frac{c_2 \overline{v}_{ax}}{2} \right) \qquad [\frac{J}{m/s}], \text{ (A.8)}$$

$$\frac{\partial W_{wheel}}{\rho} = \frac{S}{2} (c_1 \overline{v}_{ax}^2 + c_2 |\overline{v}_{wy}| \overline{v}_{ax} + c_3 \overline{v}_{wy}^2) \qquad [\frac{J}{\frac{kg}{m^3}}], \text{ (A.9)}$$

$$\frac{\partial W_{wheel}}{c_{r_{road}}} = mgc_{r_{nom}} S_h \qquad [\frac{J}{-}]. \text{ (A.10)}$$

The sensitivities are apparently dependent on both vehicle and environmental parameters. To be able to compare the relative parameters sensitivities three vehicles, a car, a rigid truck without a trailer, and a tractor with a semi-trailer combination are used as example vehicles. The sensitivity calculations are exemplified in road weather conditions according to:
$\rho = 1.21 \left[\frac{kg}{m^3}\right]$, $\overline{v}_{wx} = 0 \left[\frac{m}{s}\right]$, $\overline{v}_{wy} = 2 \left[\frac{m}{s}\right]$, $\overline{v}_{ax} = v_{ax}(0) = v_{ax}(S) = 25 \left[\frac{m}{s}\right]$ $h_r(S) = h_r(0)$, $S = S_h = 1$, $c_{r_{road}} = 1$, D = 1.

Evaluation of the formulas in equation A.2-A.10 gives the relative estimation for the three different vehicles in some typical environmental conditions according to Tables A.1-A.6.

Parameter	Nominal Value	Parameter sensitivity value	Parameter relative sensitivity value
m	1800 [kg]	0.093 [J/(m*kg)]	1.68 [J/(m*%)]
c_1	0.79 [m^2]	378 [J/m^3]	2.97 [J/(m*%)]
c_2	0.62 [m^2]	30.2 [J/m^3]	0.19 [J/(m*%)]
$c_{r_{nom}}$	0.0095 [-]	17700 [J/m]	1.68 [J/(m*%)]

Table A.1: Energy conversion losses sensitivity for car parameters.

Table A.1 shows that a car has three parameters that affect energy conversion losses a lot, i.e. the vehicle mass, m, the nominal air drag coefficient, c_1 and the nominal rolling resistance coefficient, $c_{r_{nom}}$. In a similar way, Table A.2 shows that the important environmental parameters are the headwind speed, $\overline{v}_{wx}$, the air density, ρ and the road surface conditions, $c_{r_{road}}$. Crosswinds only have a minor effect on cars. Note that even though air density is

Parameter	Nominal Value	Parameter sensitivity value	Parameter relative sensitivity value
$\overline{v}_{wx}$	0 [m/s]	24.6 [J/(m*m/s)]	1.23 [J/(m*%)] (base = 5 [m/s])
$\overline{v}_{wy}$	2 [m/s]	9.38 [J/(m*m/s)]	0.47 [J/(m*%)] (base = 5 [m/s])
ρ	1.21 kg/m^3	262 [J/(kg/m^3)]	3.17 [J/(m*%)]
$c_{r_{road}}$	1 [-]	168 [J/m]	1.68 [J/(m*%)]

Table A.2: Energy conversion losses sensitivity for environmental parameters for a car.

the most sensitive environment parameter, it is less volatile than for example the wind speeds which makes its effect on vehicle range somewhat more predictable.

Parameter	Nominal Value	Parameter sensitivity value	Parameter relative sensitivity value
m	10000 [kg]	0.055 [J/(m*kg)]	5.49 [J/(m*%)]
c_1	6.63 [m^2]	378 [J/m^3]	25.1 [J/(m*%)]
c_2	12.24 [m^2]	30.2 [J/m^3]	3.70 [J/(m*%)]
c_3	-4.59 [m^2]	2.42 [J/m^3]	0.11 [J/(m*%)]
$c_{r_{nom}}$	0.0056 [-]	98100 [J/m]	5.49 [J/(m*%)]

Table A.3: Energy conversion losses sensitivity for rigid truck parameters.

Parameter	Nominal Value	Parameter sensitivity value	Parameter relative sensitivity value
$\overline{v}_{wx}$	0 [m/s]	215 [J/(m*m/s)]	10.8 [J/(m*%)] (base = 5 m/s)
$\overline{v}_{wy}$	2 [m/s]	174 [J/m]	9.81 [J/(m*%)] (base = 5 m/s)
ρ	1.21 [kg/m^3]	2369 [J/kg/m^3]	28.7 [J/(m*%)]
$c_{r_{road}}$	1 [-]	549 [J/m]	5.49 [J/(m*%)]

Table A.4: Energy conversion losses sensitivity for environmental parameters for a rigid truck.

Comparing the rigid truck parameter's sensitivities in Table A.3 and Table A.4 with the corresponding values for a car, Table A.1 and Table A.2, show that a rigid truck is much more sensitive to crosswinds and hence also to the c_2 parameter describing the cross-sensitive air drag. The direct crosswind parameter c_3 has little influence on the energy conversion losses and may therefore be difficult to estimate based only on energy consumption measurements.

Parameter	Nominal Values	Parameter sensitivity value	Parameter relative sensitivity value
m	34000 [kg]	0.052 [J/(m*kg)]	17.68 [J/(m*%)]
c_1	5.06 [m^2]	378 [J/m^3]	19.1 [J/(m*%)]
c_2	34.04 [m^2]	30.2 [J/m^3]	10.3 [J/(m*%)]
c_3	-7.64 [m^2]	2.42 [J/m^3]	0.18 [J/(m*%)]
$c_{r_{nom}}$	0.0053 [-]	333540 [J/m]	17.68 [J/(m*%)]

Table A.5: Energy conversion losses sensitivity for tractor with semitrailer combination parameters.

Parameter	Nominal Values	Parameter sensitivity value	Parameter relative sensitivity value
$\overline{v}_{wx}$	0 [m/s]	194 [J/(m*m/s)]	9.71 [J/(m*%)] (base = 5 m/s, not 0 here)
$\overline{v}_{wy}$	2 [m/s]	496 [J/(m*m/s)]	26.67 [J/(m*%)] (base = 5 m/s, not 0 here)
ρ	1.21 [kg/m^3]	2417 [J/(kg/m^3)]	29.25 [J/(m*%)]
$c_{r_{road}}$	1 [-]	1770 [J/m]	17.68 [J/(m*%)]

Table A.6: Energy conversion losses sensitivity for environmental parameters for a tractor with semitrailer combination.

Due to its large body and high vehicle mass, the figures in Table A.5 and Table A.6 reveal that the tractor-semitrailer combination is highly sensitive to most of the included parameters. Only the direct crosswind sensitivity parameter c_3 has low sensitivity. Note also that the sensitivity on crosswind speed is significantly higher than the sensitivity on headwind speed.